Fe^{2+} and Phosphate Interactions in Bacterial Ferritin from *Azotobacter vinelandii*

Gerald D. Watt*
Department of Chemistry and Biochemistry, Brigham Young University, Provo, Utah 84602
Richard B. Frankel
Department of Physics, California State Polytechnic University, San Luis Obispo, California 94307
Deloria Jacobs
Battelle Memorial Institute, 505 King Avenue, Columbus, Ohio 45321
Heqing Huang
Department of Biology, Xiamen University, Xiamen, The People's Republic of China
Georgia C. Papaefthymiou
F. Bitter National Magnet Laboratory, Massachusetts Institute of Technology, Cambridge, Massachusetts 02139
Received January 10, 1992; Revised Manuscript Received March 26, 1992

ABSTRACT: Fe^{2+} binding to both apo- and holo- bacterial ferritin from *Azotobacter vinelandii* (AVBF) was measured as a function of pH under carefully controlled anaerobic conditions. Fe^{2+} binding to apo-AVBF is strongly pH dependent with 25 Fe^{2+} ions/apo-AVBF binding tightly at pH 5.5 and over 150 Fe^{2+}/apo-AVBF at pH 9.0. Holo-AVBF gave a similar pH-dependent binding profile with over 400 Fe^{2+}/AVBF binding at pH of 9.0. Proton release per Fe^{2+} bound to either AVBF protein increases with increasing pH until a total of about two protons are released at pH 9.0. These binding results are both qualitatively and quantitatively different from corresponding measurements (Jacobs et al., 1989) on apo- and holo- mammalian ferritin (MF) where less Fe^{2+} binds in both cases. The high level of Fe^{2+} binding to holo-AVBF relative to that of mammalian ferritin is a consequence of the higher phosphate content in the core of AVBF. Reduction of AVBF by either dithionite or methyl viologen in the absence of chelating agents demonstrated that phosphate, but not Fe^{2+}, is released from the AVBF core in amounts comensurate with the degree of iron reduction, although even at 100% reduction considerable phosphate remains associated with the reduced mineral core. Fe^{2+} binding to holo-AVBF made deficient in phosphate was lower than that of native AVBF, while the addition of phosphate to native holo-AVBF increased the Fe^{2+} binding capacity. These results clearly support the role of phosphate as the site of interaction of Fe^{2+} with the AVBF mineral core. Mossbauer measurements of $^{57}Fe^{2+}$ bound to holo-AVBF under controlled anaerobic conditions indicate that the bound Fe^{2+} undergoes a reversible electron-transfer reaction with the mineral core iron and forms $^{57}Fe^{3+}$, presumably bound to the mineral core surface. The phosphate present on the mineral core is involved in catalyzing this internal electron-transfer reaction, a process which may be an important step in bacterial ferritin mineral core development.

Bacterial ferritin from *Azotobacter vinelandii* (AVBF) is a multisubunit protein that stores large amounts of iron within its protein interior (Bulen et al., 1973; Stiefel & Watt, 1979; Watt et al., 1986) in a manner similar to that of the well-studied mammalian ferritin (MF) protein and, by analogy, is likely to serve a similar iron storage function in bacteria. Although many similarities have been noted between the MF and bacterial ferritin (BF) proteins in general (Stiefel & Watt, 1979; Watt et al., 1986; Yariv et al., 1981) and AVBF in particular, there are significant differences between these ferritin proteins. For example, AVBF contains one protoporphyrin IX heme group per pair of subunits (12 hemes per 24 subunits) whereas native MF does not. AVBF also contains a more structurally disordered mineral core containing phosphate/iron levels near 1 (Watt et al., 1986; Frankel et al., 1987; Rohrer et al., 1990), in contrast to MF where this ratio is about 0.1. In addition, the reduction properties of AVBF differ from those of MF not only by virtue of the low potential heme groups but also by a much lower reduction potential of the mineral core (Watt et al., 1986), a consequence, presumably, of the different structural and compositional properties of the phosphate-rich AVBF mineral core. Thus, while nature seems to have evolved a general overall structural strategy for storing iron as mineral cores within the multisubunit ferritin proteins, the different ferritin properties noted above probably result from evolutionary adaptations made on this theme in order to control cellular iron flux under diverse physiological conditions. Elucidation of electron-transfer processes and Fe^{2+}, Fe^{3+}, phosphate, and protein interactions are essential for understanding the processes of iron uptake, storage, and release by the different ferritin proteins.

The deposition of iron in MF under oxidizing conditions has been well studied (Clegg et al., 1980; Chasteen & Theil, 1982; Bakker & Boyer, 1985; Wardeska et al., 1985; Bauminger et al., 1989; Yang et al., 1987; Cheng & Chasteen, 1991), and several distinct ferric species have been identified as intermediates in mineral core formation. The binding of ferrous ions to MF under anaerobic conditions also has been studied (Jacobs et al., 1989). In the pH range 6.0–7.5, eight ferrous ions bind to apo-MF, a stoichiometry consistent with one ferrous binding site per 3-fold channel (Wardeska et al., 1985). These channels were recently identified as the likely sites of iron entry into apo-MF (Stefanini et al., 1989).

In contrast to small numbers of Fe^{2+} that bind to apo-MF, up to 300 ferrous ions bind anaerobically to holo-MF, most of them presumably bound to sites on the surface of the mineral core. Mossbauer spectroscopy showed that Fe^{2+}

0006-2960/92/0431-5672$03.00/0

binding to the mineral core of holo-MF was accompanied by electron transfer to ferric ions in the core (Jacobs et al., 1989).

Treffry and Harrison (1978) studied incorporation and release of inorganic phosphate by MF and found that phosphate was released ahead of iron upon thioglycolate reduction. Their results suggested that inorganic phosphate in MF is surface bound to the mineral core. The role of phosphate in initial iron deposition in apo-MF was reported to accelerate the oxidation of ferrous ions by molecular oxygen and to facilitate migration of ferric ions from an oxidation site on the protein (ferroxidase center) to the core (Cheng & Chasteen, 1991). A putative ferroxidase center has been identified in human liver H-chain ferritin but is absent in human liver L-chain ferritin (Lawson et al., 1989).

In contrast to MF, BF is less well studied. The high phosphate content of BF is apparently associated with the more amorphous or disordered mineral core structures (Mansour et al., 1985; Moore et al., 1986; Mann et al., 1987). In general, the higher the phosphate content, the greater the structural disorder of the mineral core (Mann et al., 1986). EXAFS results show that phosphate is distributed throughout the mineral core in AVBF (Rohrer et al., 1990). In MF reconstituted in the presence of excess phosphate, phosphate was also found to be distributed throughout the mineral core (Rohrer et al., 1987).

The different amino acid sequences in apo-MF and apo-AVBF (Grossman et al., 1992) and the different phosphate contents and structures of the cores in holo-MF and holo-AVBF suggest that different Fe^{2+}-binding properties and phosphate interactions are likely to be found when these two ferritin types are compared. Such a comparison of Fe^{2+}-binding ability will be of interest in understanding how both ferritin types interact with Fe^{2+} prior to oxidation to Fe^{3+} and subsequent core formation. In this paper, we report on Fe^{2+} binding to apo- and holo-AVBF as a function of pH under anaerobic conditions and on the role of phosphate in binding Fe^{2+} to holo AVBF. Mossbauer spectroscopy has been used to monitor the fate of the bound Fe^{2+}. Our results indicate that phosphate is mobilized from the AVBF mineral core upon reduction and presumably that phosphate is essential in binding Fe^{2+} to the AVBF mineral core surface in holo-AVBF. Once Fe^{2+} is bound, phosphate appears to mediate Fe^{2+}–Fe^{3+} redox interconversions which may be important in the development of the mineral core in AVBF.

Materials and Methods

Preparation of AVBF. Various samples of three-times-crystallized AVBF containing from 1300 to 1825 iron atoms/AVBF core and 1.3 to 1.7 Fe^{3+}/phosphate were prepared from AV cells washed with, suspended in, and ruptured in 0.025 M TES buffer at pH 7.4 as previously described (Bulen et al., 1973; Watt et al., 1986). AVBF prepared by this procedure was used for the Fe^{2+}-binding measurements, the Mossbauer spectroscopy, and the phosphate variation experiments described below. A second method for preparing AVBF consisted of suspending and rupturing the AV cells in 0.05 M potassium phosphate buffer, pH 7.4, and then conducting the isolation and crystallization steps in 0.025 M TES buffer as described (Watt et al., 1986). Phosphate analysis (Cooper, 1977) for three-times-crystallized AVBF prepared by both methods revealed that the phosphate level in AVBF prepared by the second method was higher, suggesting that phosphate incorporation into the AVBF mineral core occurred during contact with phosphate ion during isolation. To examine this possibility, several independent preparations of crystallized AVBF prepared by the first method (in the absence of phosphate) were analyzed for phosphate and then incubated for 30 min with 0.1 M potassium phosphate at pH 7.5, and finally 150-μL portions were passed through a 1 × 15 cm Sephadex G-25 column to remove unbound phosphate. The resulting AVBF samples were crystallized and analyzed for phosphate. The described treatment resulted in an increase in the phosphate content of AVBF (see Table I), demonstrating that additional phosphate was incorporated, presumably into the AVBF mineral core. Most experiments described below utilized the "native" AVBF prepared in the absence of additional phosphate, unless otherwise noted.

Anaerobic Conditions. The reactions to be described utilize very air-sensitive reductants to form air-sensitive Fe^{2+} intermediates of AVBF. In order to unequivocally evaluate their redox reactivity, it is necessary to exclude the possibility of inadvertant oxidation. All air-sensitive reactions involving AVBF were carried out in a Vacuum Atmospheres glove box containing nitrogen or argon (O_2 < 1 ppm). The Mossbauer samples were prepared in the glove box, sealed in air-tight containers, and removed and quickly frozen in liquid nitrogen.

Phosphate Variation in AVBF Mineral Cores. Phosphate loss from AVBF to produce phosphate-altered mineral cores was carried out by two separate procedures. The first consisted of reducing various samples (0.2–0.5 mL) of anaerobic AVBF (10–15 mg/mL) by 10% increments from 0 to 50% and then by 100% with reduced methyl viologen (MV) (Corbin & Watt, 1990) for 30–60 min, followed by anaerobic chromatography on a 1.0 × 15 cm Sephadex G-25 column to remove the MV components, free phosphate ion, and any released iron. Iron (Lovenberg et al., 1963), phosphate (Cooper, 1977), and protein (Lowry) analyses before and after reduction and chromatography demonstrated that phosphate but little iron was lost from the AVBF core. The effluent from the column, following the emergence of the protein, was also analyzed for iron and phosphate to determine more precisely the free iron and phosphate released upon reduction.

The same reduction protocol was used for the second procedure except that bipyridine was added to chelate Fe^{2+} and release the phosphate bound to the reduced AVBF core. Both iron and phosphate are released in near equal amounts in this process. Iron and phosphate were measured before and after reduction and chelation to characterize the resulting AVBF cores.

Fe^{2+} Binding and H^+ Release. Anaerobic Fe^{2+} binding to both apo- and "native" holo-AVBF as a function of pH was conducted by the Sephadex G-25 method used previously for the MF system (Jacobs et al., 1989). Holo-AVBF from which phosphate (but not iron) was removed as described above was used to determine the effect of phosphate loss on Fe^{2+} binding to holo-AVBF. Holo-AVBF to which additional phosphate was added and from which the excess was removed by Sephadex G-25 chromatography was also examined for its Fe^{2+}-binding ability relative to that of "native" holo-AVBF.

Proton release accompanying Fe^{2+} binding to both apo- and native holo-AVBF was conducted as a function of pH as previously described (Jacobs et al., 1989), using AVBF which had been dialyzed against 0.15 M NaCl to remove all buffering components. Specially prepared MV (Corbin & Watt, 1990), free from small chelating molecules, was used because reduction by this reagent occurs with no net proton transfer accompanying electron transfer.

Mossbauer Spectroscopy. Iron-57 metal enriched to 95% (New England Nuclear–Du Pont) was dissolved in 0.01 M H_2SO_4 (50–70 °C) under anaerobic conditions to produce $^{57}Fe^{2+}$ at concentrations of 0.01–0.1 M at pH 5–6.5. $^{57}Fe^{3+}$

was well below 1% of the total iron present. $^{57}Fe^{2+}$ was added anaerobically in stoichiometric amounts (as determined from the binding experiments described above) to apo- and holo-AVBF at 10–16 mg/mL at pH 7.5, the solution was incubated 30 min, and then an aliquot of each ferritin fraction was reacted with bipyridine to determine the Fe^{2+}/ferritin ratio and to verify that the bound iron had not undergone net oxidation.

Apo-AVBF samples prepared in this manner are summarized in Table II as apo-AVBF(1), which contained $^{57}Fe^{2+}$ bound at pH 7.0, and apo-AVBF with $^{57}Fe^{2+}$ bound at pH 9.0.

Holo-AVBF samples with $^{57}Fe^{2+}$ bound at pH 7.0 and 9.0 were divided into two portions. One portion was loaded into air-tight plastic containers and frozen. The other portion was exposed to air for over an hour to oxidize the bound Fe^{2+} and then made anaerobic and incubated with excess nonisotopically enriched Fe^{2+} (2.2% $^{57}Fe^{2+}$) for 30 min. After anaerobic Sephadex G-25 chromatography, the sample was loaded into an air-tight sample holder and frozen. An aliquot was taken before loading to verify that the iron added in the second binding step was all in the Fe^{2+} state. Table II summarizes the four holoferritin samples that were prepared: holo-AVBF(1), containing added 95% $^{57}Fe^{2+}$ at pH 7.0; holo-AVBF(2), with 2.2% $^{57}Fe^{2+}$ bound anaerobically at pH 7.0, following binding of 95% $^{57}Fe^{2+}$ at pH 7.0 and air oxidation; holo-AVBF(3) with 95% $^{57}Fe^{2+}$ bound at pH 9.0; and holo-AVBF(4) with 2.2% $^{57}Fe^{2+}$ bound anaerobically at pH 9.0 following binding of 95% $^{57}Fe^{2+}$ at pH 9.0 and air oxidation.

Mossbauer spectra for each of the AVBF samples were obtained with a variable temperature cryostat and a constant acceleration Mossbauer spectrometer at a number of temperatures between 4.2 and 250 K. Spectra were analyzed with a least-squares fitting program to yield isomer shifts, quadrupole splittings, magnetic hyperfine splittings, and relative intensities of spectral components. Isomer shifts were measured with respect to iron metal at 300 K.

Results

Fe^{2+} Binding to Apo-AVBF. Figure 1A is a plot of Fe^{2+} bound to apo-AVBF as a function of pH. These data were obtained by reaction of apo-AVBF with excess Fe^{2+} at the indicated pH, removing excess, unbound Fe^{2+} by anaerobic Sephadex G-25 chromatography and then measuring the Fe^{2+} associated with ABVF. The addition of less than the stoichiometric amount of Fe^{2+} resulted in only Fe^{2+} present in the protein fraction, a result indicating that Fe^{2+} is strongly attached to AVBF. Meaningful results were not obtained below pH 5.5 because protein precipitation occurred near the isoelectric point or above pH 9.0 where irreproducible behavior was observed, probably due to $Fe(OH)_2$ formation. A nearly linear increase in the number of Fe^{2+} bound to AVBF with pH was measured, ranging from 25 at pH 5.5 to 160 at pH 9.0, where Fe^{2+} binding appeared to level off. The pH-dependent Fe^{2+}-binding behavior in Figure 1A indicates that protons are released when Fe^{2+} binds to anaerobic apo-AVBF. This was confirmed by the directly measured values shown as the right axis in Figure 1A. Fe^{2+} binding at all pH values investigated was reversible to Fe^{2+} removal either by pH adjustment to lower values, where bound Fe^{2+} is released as indicated by Figure 1A, or by quantitative Fe^{2+} removal by the bipyridine chelating agent. These results confirm that anaerobic conditions have been maintained and that Fe^{2+} and *not* Fe^{3+} interactions are being measured in Figure 1A.

In order to demonstrate that the results in Figure 1A do not arise from residual iron still present in AVBF, an additional iron removal step was included. The reduction of apo-AVBF

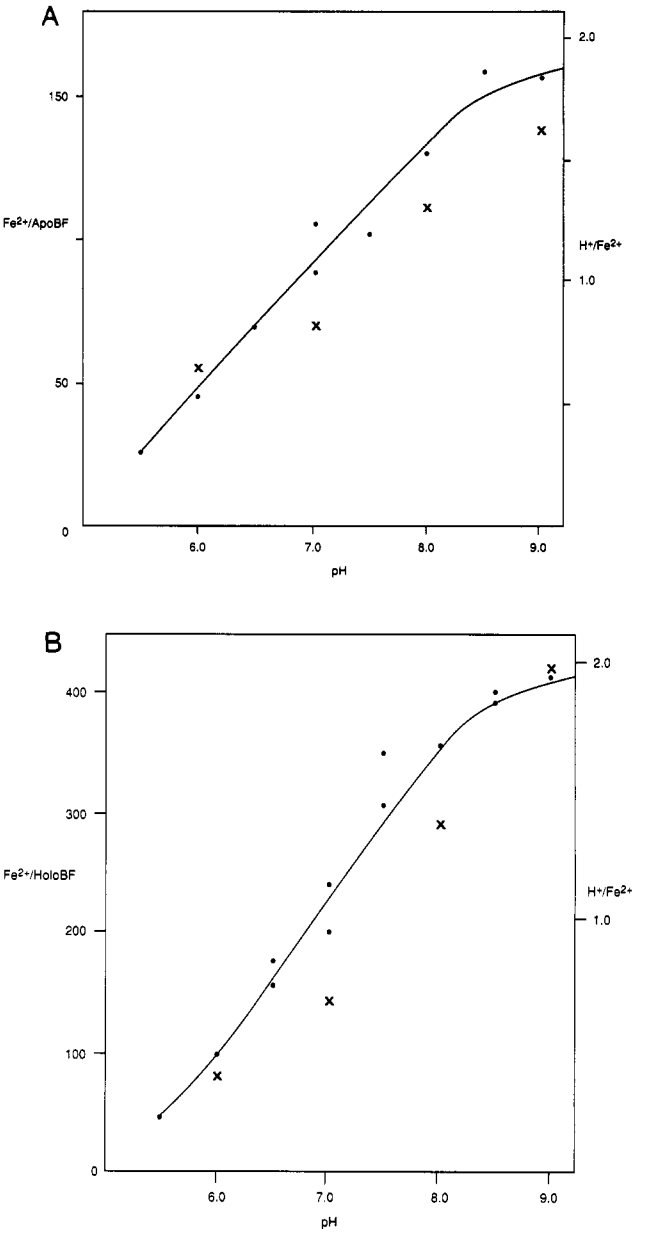

FIGURE 1: (A) Fe^{2+} binding to apo-AVBF as a function of pH. The left axis is the number of Fe^{2+} ions bound (·) at the indicated pH. The right axis is the number of protons released per Fe^{2+} bound (×). (B) The left axis is the number of Fe^{2+} bound to holo-AVBF (·) containing 1520 iron atoms and 1143 phosphate groups per AVBF molecule as a function of pH. The right axis is the number of protons released per Fe^{2+} bound (×) at the indicated pH.

with MV or dithionite followed by addition of bipyridine and finally chromatography on Sephadex G-25 produced apo-AVBF with no detectable core iron present (the iron in the heme groups was still present) but which bound Fe^{2+} as shown in Figure 1A. We conclude that the Fe^{2+}-binding profile in Figure 1A is an inherent property of apo-AVBF.

Fe^{2+} Binding to Holo-AVBF. Figure 1B is a plot of Fe^{2+} bound to holo-AVBF under anaerobic conditions as a function of pH for AVBF containing 1520 Fe/AVBF. In other AVBF samples with 1350 and 1835 Fe/AVBF, the Fe^{2+}-binding stoichiometry at pH 9.0 was 395 and 435, respectively compared to the value of 412 shown in Figure 1B. As with apo-AVBF, Fe^{2+} binding is pH dependent through the pH range from 5.5 to 9.0, but the degree of binding at a given pH is much greater with holo- than with apo-AVBF. This increase in binding capacity of holo-AVBF compared to that of apo-AVBF is directly attributable to the phosphate-rich mineral

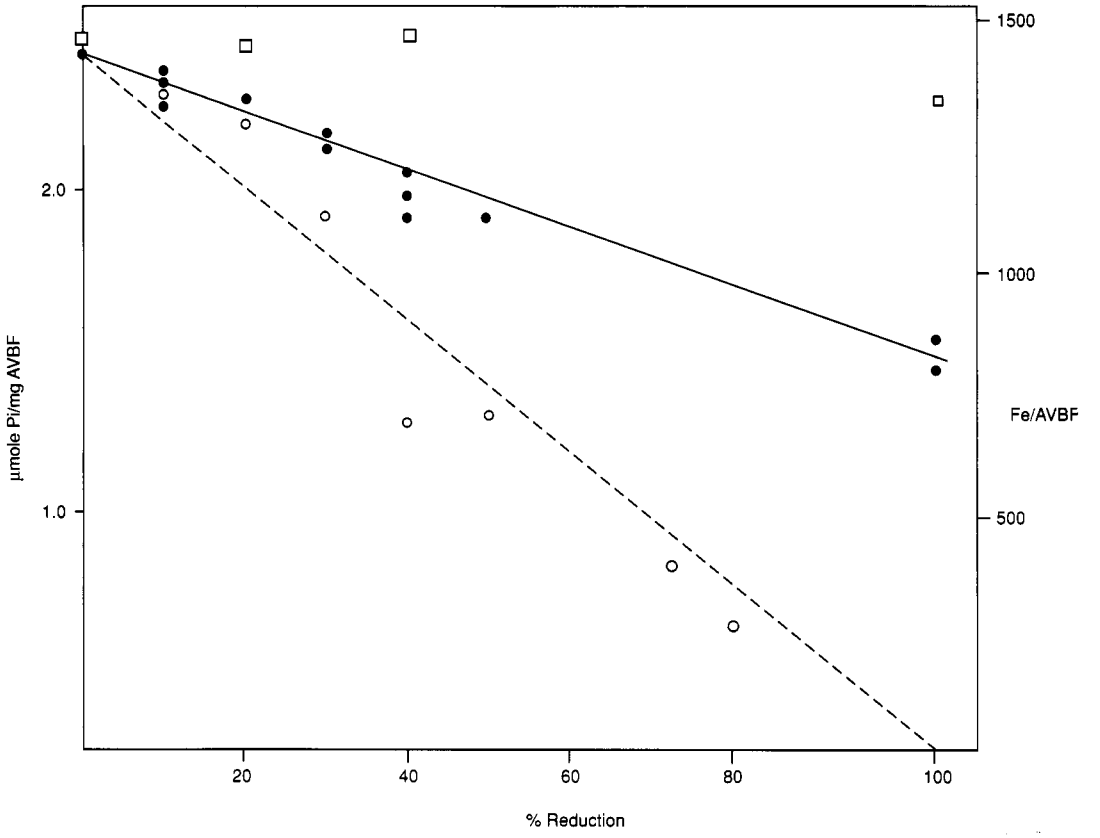

FIGURE 2: Phosphate release upon reduction of holo-AVBF with reduced MV. The solid line is a linear fit to the phosphate content (●) present in the holo-AVBF reduced core after the indicated percentage of reduction of AVBF with MV followed by anaerobic Sephadex G-25 chromatography. The iron content of the AVBF core (□) was determined following the above reduction and chromatography steps. The dashed line of the lower curve is the predicted and the points (○) are the measured phosphate content for holo-AVBF after core reduction followed by removal of the resulting Fe^{2+} by bypyridine chelation.

core present in holo-AVBF. The large variation in Fe^{2+} binding to anaerobic holo-AVBF with pH indicates that proton release accompanies Fe^{2+} binding, as shown experimentally on the right axis of Figure 1B. Up to two protons are released as Fe^{2+} binds at pH 9.0. The reversibility of Fe^{2+} binding to holo-AVBF was essentially complete as evidenced by reaction with excess bipyridine which released the added Fe^{2+} as the bipyridine complex.

Phosphate Addition to the AVBF Mineral Core. AVBF isolated in the presence of phosphate at pH 7.5 has a higher phosphate content than that isolated in the absence of added potassium phosphate. This result, shown as sample 6 in Table I, has been observed in several independently prepared AVBF samples and suggests the presence of phosphate binding sites presumably in the native AVBF mineral core which bind additional phosphate during the isolation steps. This proposal was confirmed by incubating purified "native" AVBF with phosphate, separating the holo-AVBF from the excess phosphate and measuring elevated phosphate levels in the AVBF core. Typically, a 10–15% increase in the AVBF phosphate content is observed. For example, two independent, "native" holo-AVBF samples with initial phosphate values of 1.30 and 1.41 μmol of phosphate/mg of AVBF increased to 1.58 and 1.72 μmol of phosphate/mg of AVBF, respectively, corresponding to an increase in the P_i/iron ratio from 0.7 to 0.95. The various methods that were used to remove excess phosphate and the repeatability of the procedure when applied to several independently prepared AVBF samples give confidence that phosphate incorporation is a property of the native AVBF mineral core.

Phosphate Release from the Holo-AVBF Core. Phosphate release from the mineral core was accomplished by two procedures: one which leaves the iron content of the AVBF core essentially unchanged while the other modifies both the iron and phosphate core content. Figure 2 summarizes the results from both types of experiments. The middle set of data connected by the solid line shows that only phosphate is released when AVBF is reduced to varying extents with MV and the protein separated by Sephadex G-25 chromatography. Phosphate loss varies nearly linearly with the extent of reduction but even at 100% reduction a rather large amount of phosphate is retained by the reduced mineral core. The upper points (right axis) demonstrate that iron loss is minimal (2–5% loss) during this treatment. These results establish that phosphate but not Fe^{2+} is easily lost from the reduced or

Table I: Phosphate and Iron Content of Native and Altered AVBF[a]

sample	Fe/ AVBP	% reduced	P_i (μmol/mg)	P_i/AVBF	Fe^{2+}/ AVBF
1	1350	0	2.17	955	290[e]
2	1295	30	1.90	836	258
3	1270	45	1.65	726	194
4	945[b]	30	1.71	752	188
5	625[b]	45	0.92	405	125
6	1350[c]	0	2.40	1056	325
7	1350[d]	0	2.17		223

[a] The native AVBF with the indicated iron and phosphate content is shown as sample 1. For samples 2–7, the native AVBF was reduced as indicated in column 3 and the resulting AVBF was reanalyzed for iron and phosphate. The last column is the Fe^{2+} bound to the resulting AVBF. [b] Reduced as indicated, but Fe was removed by bipyridine chelation and separated by anaerobic Sephadex G-25 chromatography prior to Fe^{2+} addition. [c] Same as sample 1 except additional phosphate was stoichiometrically bound to AVBF prior to Fe^{2+} addition. [d] Same as sample 1 except 2 mM phosphate was present when Fe^{2+} was added. [e] Replicate measurements gave an uncertainty of ±10 Fe^{2+}/AVBF.

Table II: Samples for Mossbauer Spectroscopy of Apo-AVBF and Holo-AVBF[a]

sample	pH	original $^{57}Fe^{3+}$	step 1, added $^{57}Fe^{2+}$ [b]	step 2, added $^{57}Fe^{2+}$ [c]	net $^{57}Fe^{2+}/^{57}Fe^{3+}$
holo(1)	7.0	42.5	155[d]	0	155/42.5
holo(2)	7.0	42.5	155[d]	3.6[f]	3.6/197.5
holo(3)	7.0	42.5	382[e]	0	382/42.5
holo(4)	9.0	42.5	382[e]	8.8[f]	8.8/424.5
apo(1)	7.0	0	87	0	87/0
apo(2)	9.0	0	124	0	124/0

[a] The AVBF samples were prepared by anaerobic binding of ferrous ions to apo-AVBF ferritin and to holo-AVBF ferritin containing an average of 1931 ferric ions/molecule distributed as 42.5 $^{57}Fe^{3+}$ and 1888.5 $^{56}Fe^{3+}$ (natural isotopic ratio). [b] Fe^{2+} isotopically enriched to 95% ^{57}Fe. [c] Fe^{2+} with natural (2.2%) ^{57}Fe. [d] Total Fe^{2+} bound = 163. [e] Total Fe^{2+} bound = 402. [f] Added following oxidation of all iron added in step 1.

partially reduced AVBF mineral core. Even at 100% core reduction, about 50% of the original phosphate is still present in the Fe^{2+} core. It is not clear whether this phosphate is thermodynamically stable or is just physically trapped within the Fe^{2+} mineral phase.

If the partially reduced AVBF (which has had its mobilized phosphate removed) is reoxidized, incubated with 5 mM phosphate, and then reisolated by Sephadex G-25 chromatography, there is no significant phosphate reincorporation into the mineral core. This result demonstrates that once reduction has released the Fe^{3+}-bound phosphate and the released phosphate is separated from the core, oxidation of the resulting Fe^{2+} back to Fe^{3+} produces a new environment (presumably oxo and hydroxo ligands bound to Fe^{3+}) which satisfies the coordination requirements of Fe^{3+}. Once this new and presumably more stable environment forms around Fe^{3+}, phosphate cannot compete as a ligand and therefore it does not bind to the altered AVBF core. These results imply that during iron deposition into AVBF, the phosphate and iron enter the core together to form the phosphate–Fe^{3+} mineral core. If iron entered first, it would likely form stable FeOOH into which phosphate will not enter once the oxo–hydroxo environment around Fe^{3+} is formed.

Reduction of AVBF with MV followed by chelation of the resulting Fe^{2+} releases both reduced iron and phosphate in a near one to one ratio. This result is expected from the near one to one composition ratio of iron to phosphate present in the AVBF core and is shown by the dashed line in Figure 2. At reduction values of 10% and 20%, the phosphate remaining within the core more closely parallels the middle curve (reduction only) than that predicted by the lower curve. The scatter in the data of the lower curve makes it difficult to draw precise conclusions, but it appears that some of the phosphate released upon Fe^{2+} chelation becomes bound to phosphate-deficient sites already present or that are produced during the reduction and chelation step in a manner similar to that observed in native AVBF.

Fe^{2+} Binding to Phosphate Altered AVBF Cores. Table I summarizes Fe^{2+}-binding experiments to native holo-AVBF and to holo-AVBF modified by (1) binding additional phosphate to the mineral core; (2) removal of phosphate by reduction only; or (3) partial removal of AVBF core by reduction and Fe^{2+} chelation. These results are typical of experiments conducted with other independently prepared AVBF samples. The addition of phosphate to the mineral core enhances the Fe^{2+}-binding ability of holo-AVBF as is seen in Table I by comparing the number of Fe^{2+} bound (325) in sample 6 with that (290) in sample 1. In contrast, Table I also shows that the Fe^{2+}-binding capacity decreases with decreasing phosphate levels in the AVBF core (compare samples 2 and 3 with 1), even though the core size, as evidenced by the iron content, remains constant. Table I further shows (sample 7) that the presence of free phosphate (at 2 mM) decreases the Fe^{2+}-binding capacity of holo-AVBF even though additional phosphate has presumably bound to sites in the core (as in sample 6) which should increase the Fe^{2+}-binding ability. The presence of free phosphate probably successfully competes with the surface-bound phosphate groups in chelating the incoming Fe^{2+} ions which decreases the overall AVBF binding capacity. When taken together, the results strongly support the conclusion that incoming Fe^{2+} ions bind to surface-exposed phosphate groups.

The number of phosphate groups, presumably on the AVBF core surface, required to bind each incoming Fe^{2+} can be estimated from the results in Table I by comparing the results in the last column (the number of Fe^{2+} bound per holo-AVBF) with column 5 (the number of phosphate groups present in holo-AVBF). This comparison shows that samples 2 and 3 have 119 and 229 fewer phosphate groups present than sample 1 and bind 55 and 80 fewer Fe^{2+}, respectively. These results suggest that 2.16 and 2.86 phosphate groups are required for each Fe^{2+} bound under these two sets of conditions. Likewise, a comparison of sample 6 (where additional phosphate has bound) with sample 1 indicates that 45 additional Fe^{2+} bind to AVBF which has had an increase of 101 phosphate groups, a result indicating that 2.24 phosphate groups are involved in binding each Fe^{2+}.

The removal of iron and phosphate by reduction and chelation of Fe^{2+}, as shown in Figure 2, provides AVBF samples with essentially the same iron to phosphate ratios but with modified core sizes due to partial core removal. Table I shows that Fe^{2+} binding decreases dramatically with core size, a result consistent with a decrease in the surface area and hence the number of surface-bound phosphate groups on the mineral particle surface where Fe^{2+} binds. Samples 4 and 5, compared to sample 1, indicate that a 21% and a 58% loss of phosphate results in a 38% and a 57% decrease in Fe^{2+} binding, respectively. These results are consistent with the phosphate content contributing to Fe^{2+} binding but are complicated due to both phosphate and core size variation. The Fe^{2+}-binding results from both types of phosphate-altered ferritins suggest that at least two phosphate groups are required to bind each Fe^{2+} to AVBF and that these groups are likely to be on the surface of the AVBF mineral core.

Mossbauer Spectroscopy. The zero-applied magnetic field Mossbauer spectra of AVBF apo(1) and AVBF apo(2) consisted primarily of a broad-line (0.7 mm/s FWHM) ferrous quadrupole doublet (isomer shift (IS) = 1.26 mm/s, quadrupole splitting (QS) = 3.10 mm/s at 80 K) and a residual ferric doublet (IS = 0.47 mm/s at 4.2 K) accounting for 5% of the total signal intensity. Application of an 80-kOe magnetic field to AVBF apo(1) at 4.2 K resulted in a broad, asymmetric spectrum, which reflected magnetic hyperfine fields induced by the applied magnetic field at the iron nuclei, in addition to the applied magnetic field. This suggested that the Fe^{2+} ions in AVBF apo(1) are bound in the high spin state and are not magnetically ordered at 4.2 K.

The Mossbauer spectra of AVBF holo(1) at 1.5, 4.2, 7, 10, and 80 K are shown in Figure 3. The spectra of AVBF holo(2), AVBF holo(3), and AVBF holo(4) were similar, and all spectra could be decomposed into ferric and ferrous subspectra. The ferrous subspectrum consisted of a broadened quadrupole doublet at all temperatures. The ferric subspectrum exhibited the superparamagnetic transition char-

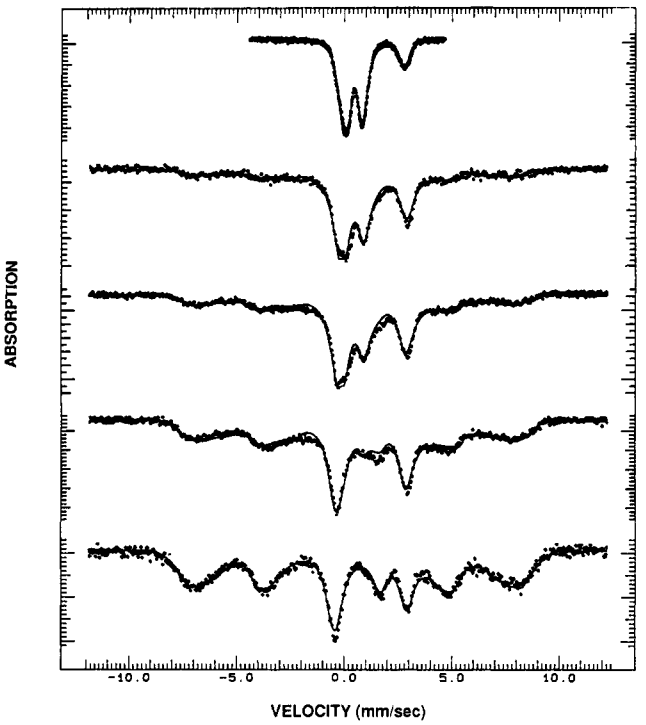

FIGURE 3: Mossbauer Spectra of AVBF holo(1) at 80, 10, 7, 4.2, and 1.5 K (top to bottom). The solid lines are theoretical least-squares fits to the experimental data.

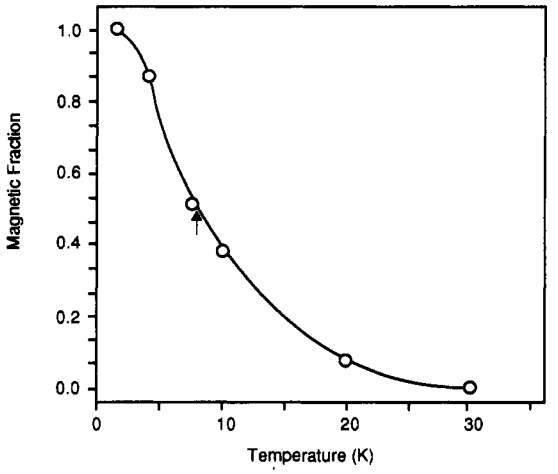

FIGURE 4: Magnetic sextet fraction of the ferric subspectrum in AVBF holo(1). The magnetic fraction is defined as the area under the sextet ferric subspectrum divided by the total area under the combined ferric subspectrum (O). The solid line connects the data points. The arrow indicates the blocking temperature of 7.5 K.

acteristic of fully oxidized AVBF holoferritin (Watt et al., 1986) with a magnetic hyperfine split sextet at 4.2 K (magnetic hyperfine field distribution mode = 485 kOe) and a quadrupole doublet above 25 K. Between 4.2 and 25 K, the ferric doublet and sextet were superposed with relative intensities that were temperature dependent (Figure 4). By definition, the average supermagnetic blocking temperature $\langle T_B \rangle$ is the temperature at which the doublet and sextet have equal spectral intensities. The average blocking temperatures were 7.5, 9.3, 10, and 12 K for AVBF holo(1), AVBF holo(2), AVBF holo(3), and AVBF holo(4), respectively. In every holo-AVBF sample, $\langle T_B \rangle$ was less than the average blocking temperatures of fully oxidized AVBF with 1000 iron atoms/molecule ($\langle T_B \rangle$) and that of AVBF electrochemically reduced 80% ($\langle T_B \rangle > 20$ K) (Watt et al., 1986).

As previously noted for mammalian ferritin (Jacobs et al., 1989), the total absorption area of the ferric sextet at 4.2 K

Table III: Relative Ferric and Ferrous Iron-57 Mossbauer Intensities in AVBF Holo-ferritin Samples

sample	experimental relative intensities	expected[a] relative intensities
holo(1) Fe^{2+}	0.26	0.78
Fe^{3+}	0.74	0.22
holo(2) Fe^{2+}	0.14	0.018
Fe^{3+}	0.86	0.982
holo(3) Fe^{2+}	0.25	0.90
Fe^{3+}	0.75	0.10
holo(4) Fe^{2+}	0.16	0.02
Fe^{3+}	0.84	0.98

[a] Calculated from the last column of Table II, assuming no electron exchange between added ferrous iron and ferric iron in the mineral core particle (see text).

in all AVBF holo-ferritin samples is somewhat greater than the area of the ferric doublet above 30 K. This effect is not due to the temperature dependence of the recoilless fraction because the latter is practically temperature invariant below 80 K. Since these were "thin" absorbers (total absorption intensities of only a few percent), differential saturation effects in the two spectra, with the sextet lines less saturated than the doublet lines (Greenwood & Gibb, 1971), cannot account for the effect. We are currently investigating the possibility that there are changes in the recoilless fraction associated with the superparamagnetic transition (M. E. Mohie-Eldin et al., unpublished results). In any case, this effect has minimal bearing on the determination of the superparamagnetic blocking temperatures.

In spectra obtained between 80 and 200 K, the ferrous absorption area of the ferrous doublet decreased faster with increasing temperature than the ferric doublet absorption area. This is similar to the temperature dependences of the absorption areas of the respective doublets in partially reduced ferritin (Watt et al., 1986). The absorption area of the ferric doublet in all of the holo-AVBF samples had a temperature dependence similar to that of fully oxidized ferritin. The ferrous doublet had a temperature dependence of the absorption area similar to that of AVBF apo(1) and AVBF apo(2).

Internal Redox Reaction of Fe^{2+} Bound to Holo-AVBF. The relative absorption areas of the ferric and ferrous doublets for the holo-AVBF samples are shown in Table III. Assuming that no net oxidation of the bound ferrous ions occurred following the initial anaerobic addition of Fe^{2+} to AVBF holo-ferritin, the ferrous and ferric absorption areas at 40 K would be proportional to the number of the respective ions with ^{57}Fe nuclei in the sample. This prediction assumes that the recoilless fractions of Fe^{3+} and Fe^{2+} are equal at 40 K. Even if the Fe^{2+} recoilless fraction in AVBF holo-ferritin were a few percent lower than the Fe^{3+} recoilless fraction at 40 K, the ferric doublet was more intense than expected in AVBF holo(1) and AVBF holo(3), whereas the ferrous doublet was more intense than expected in AVBF holo(2) and AVBF holo(4). For example, if all of the original 1931 Fe^{3+} ions/molecule in AVBF holo(1) remained Fe^{3+} and all of the 163 added Fe^{2+} ions (95% ^{57}Fe) remained Fe^{2+}, we would expect on the average for AVBF holo(1) to have 155 $^{57}Fe^{2+}$ and 42.5 $^{57}Fe^{3+}$, or ferrous and ferric relative spectral absorption areas of 0.78 and 0.22, respectively. The experimental values were 0.26 ferrous and 0.74 ferric. The result was similar for AVBF holo(3).

In AVBF holo(2), the bound Fe^{2+} ions (95% ^{57}Fe) were oxidized by exposure of the sample to air, giving an average of 197.5 $^{57}Fe^{3+}$/molecule. Subsequent addition of Fe^{2+} (2.2% ^{57}Fe) resulted in 3.6 $^{57}Fe^{2+}$/molecule. Thus, the expected

relative absorption areas were 0.018 ferrous and 0.982 ferric, whereas the experimental values were 0.14 ferrous and 0.86 ferric. The results for AVBF holo(4) were similar.

Thus, in AVBF holo(1) and AVBF holo(3), a substantial fraction of the added $^{57}Fe^{2+}$ was converted to $^{57}Fe^{3+}$, whereas in AVBF holo(2) and AVBF holo(4) a substantial fraction of the $^{57}Fe^{3+}$ bound in the core particle was converted to $^{57}Fe^{2+}$ after addition of unenriched Fe^{2+} (see Table III). These results are similar to those for mammalian ferritin (Jacobs et al., 1989). A consistent interpretation of these results is that Fe^{2+} ions, when incubated with AVBF holo ferritin under anaerobic conditions, enter the ferritin cavity, bind to the hydrous phosphoferric oxide core particle, and partially exchange electrons with the ferric ions in the core particle. In AVBF holo(2) and AVBF holo(4) this process resulted in partial reduction of $^{57}Fe^{3+}$ in the core particle by the added Fe^{2+}. The conversion of added $^{57}Fe^{2+}$ to $^{57}Fe^{3+}$ in AVBF holo(1) and AVBF holo(3) upon binding to AVBF holo-ferritin was confirmed to be an "internal oxidation" as opposed to inadvertent oxidation (by O_2, for example) by reacting an aliquot of the Fe^{2+}-bound ferritin with bipyridine and showing that the original amount of added Fe^{2+} could be recovered by bipyridine complexation. Inadvertent oxidation would have given a smaller Fe^{2+} recovery.

AVBF Mineral Core Surface. The lower average blocking temperatures of the Fe^{2+}-bound AVBF holo-ferritin samples compared to fully oxidized AVBF holo-ferritin presumably result from binding of the added Fe^{2+} to the surface of the core particle. This is also similar to the situation in mammalian ferritin (Jacobs et al., 1989). The $^{57}Fe^{3+}$ produced by oxygen or core-particle ferrous ion oxidation would be sited predominantly near or on the surface of the core particle. In the theory of superparamagnetic relaxation as applied to ferritin (Oosterhuis & Spartalian, 1976), the electronic spins of all the ferric ions in the core particle relax at the same rate, which is an exponential function of the particle volume/temperature ratio. For a given particle volume, the blocking temperature is defined as the temperature at which the spin-relaxation rate equals the Larmor precession frequency of the ^{57}Fe nucleus in the local magnetic hyperfine field. Since the surface ferric ions have about the same hyperfine field as the ferric ions in the bulk of the core particle (magnetic hyperfine field distribution mode = 490 kOe; Watt et al., 1986), the differences in the blocking temperatures cannot be explained by differences in the Larmor precession time. Several possible causes have been proposed (Jacobs et al., 1986), including formation of protoclusters by the surface ferric ions, which have smaller effective volumes than the bulk core particle with consequently lower blocking temperatures. It has also been suggested that the surface ferric ions relax at a faster rate than the bulk ions at the same temperature, especially those that are in contact with ferrous ions on the surface. It is intriguing that in the 80% reduced ferritin the bulk blocking temperature *increases* compared to in fully oxidized ferritin (Watt et al., 1986). This latter effect may arise from the massive number of surface ferrous ions on the magnetic anisotropy of the core particle (Bell et al., 1984). Alternatively, it might suggest that the arrangement of ferrous ions in the core depends on whether those ferrous ions are introduced by direct reduction of ferric ions in the core particle or by binding of ferrous ions from the external medium.

Discussion

The high phosphate content of AVBF is one of several properties of this ferritin that distinguish it from the MF protein. The high phosphate content was suggested (Watt et al., 1986) to be responsible for the greater degree of disorder of the AVBF mineral core as well as its lower reduction potential. EXAFS measurements (Rohrer et al., 1990) of the AVBF core clearly indicate that the structure of the mineral core has distinct iron–phosphate interactions, a result which follows from the approximate 1.3/1 Fe^{3+}/phosphate composition of native AVBF. However, both the preparation of AVBF in the presence of phosphate and the intentional addition of phosphate to purified native AVBF results in AVBF whose mineral core has incorporated additional phosphate (Table I). The added phosphate appears to bind to vacant sites at the mineral core, presumably at Fe^{3+} sites on the mineral core surface. The exact role of phosphate in the mineral core remains undefined but the results reported here that additional phosphate can be added to the AVBF core and that the phosphate level in the core can be varied by reduction and chelation or by reduction only provides an opportunity to investigate in more detail the role of phosphate in AVBF. Our initial investigations have centered upon the role of phosphate in anaerobically forming Fe^{2+} complexes with holo-AVBF, which may be intermediates in the core development process.

The results in Table I clearly show that increased Fe^{2+} binding to AVBF correlates with increased phosphate content while decreased Fe^{2+} binding is a consequence of decreased core phosphate levels. What is the nature of this Fe^{2+}–phosphate interaction? Little detail is provided by the binding information itself, except that two phosphate groups on the mineral core surface are probably involved in Fe^{2+} binding. The Mossbauer spectra of $^{57}Fe^{2+}$ bound to holo-AVBF demonstrate that a significant amount of the added Fe^{2+} is transformed into Fe^{3+}, presumably by electron transfer to the AVBF mineral core, as was previously reported (Frankel et al., 1987; Jacobs et al., 1989) for similar experiments on the MF system. Because the presence of phosphate is necessary for Fe^{2+} binding, it is reasonable to conclude that phosphate is somehow involved in this internal electron-transfer step. The nature of this internal electron-transfer process remains obscure but is reversible as demonstrated by the addition of bipyridine which removes the newly formed Fe^{3+} as the Fe^{2+} bipyridine chelate.

Because Fe^{3+} has a much higher affinity than Fe^{2+} for phosphate, this internal electron-transfer step may provide a means for stabilizing the incoming Fe^{2+} as surface-bound Fe^{3+} by firmly attaching the latter to the underlying, anchoring phosphate layer. The pH-dependent proton release that accompanies this Fe^{2+}-binding process (Figure 1B) probably results from the increased tendency for hydrolysis with increasing pH of the Fe^{3+} formed by internal electron transfer. Only two protons are released at pH 9 or above instead of the three expected for $Fe(OH)_3$ formation because the Fe^{3+} is partially coordinated to phosphate groups which prevents complete hydrolysis from occurring and yields only two protons per iron bound.

The proceeding hypothesis accounts for some of the observed properties that we have measured during our initial studies of Fe^{2+} binding to holo-AVBF and may form a useful starting point for visualizing the rather complex iron deposition process occurring in the holo-AVBF ferritin core. This hypothesis provokes several questions about the redox reactions involved in AVBF core development and the role of phosphate in this process. For example, by what process are the core-contained electrons (resulting from conversion of surface bound Fe^{2+} to Fe^{3+}) removed so that succeeding cycles of incoming Fe^{2+} can be accommodated? The heme groups present in AVBF may function to transfer core-bound electrons to electron acceptors

on the outside of the AVBF molecule and remove the accumulating electrons from the core. We have not observed reduced heme during Fe^{2+}-binding experiments, a result which is not surprising given previous results (Watt et al., 1986, 1988) which indicate that the heme groups are 30 mV lower in potential than the reduced core. However, if external oxidants are at a significantly higher potential than the heme groups, then electrons could be transferred from the core through the heme groups and into the external oxidant. Cytochrome *c*, $Fe(CN)_6$, and O_2 all have been shown (Watt et al., 1988) to oxidize added, core-bound Fe^{2+} ions as well as the chemically reduced core of AVBF, a result consistent with the above view.

A second question raised by the results reported here is the following: how does the new phosphate layer form in order to bind the next Fe^{2+} layer and each succeeding cycle thereafter? In other words, how does the cell coordinate the transfer of both Fe^{2+} and phosphate into the AVBF core? The results in Table I demonstrate that reoxidation of the reduced core following phosphate removal produces AVBF incapable of binding added phosphate, a result showing that the core properties have become altered toward phosphate binding. It appears then that phosphate and iron must be added together during core formation and implies that an in vivo phosphate as well as iron delivery system must function during ferritin filling. Does this conclusion suggests a phosphate storage role for AVBF in addition to its iron storage role or is phosphate incorporation into the AVBF core an adaptation that is required by the bacterial physiology in order to store iron? In vitro reconstitution studies with apo-AVBF should indicate the conditions for duplicating the native holo-AVBF mineral core and may be important in understanding how phosphate is incorporated.

The Fe^{2+}-binding behavior of apo-AVBF shown in Figure 1A stands in sharp contrast to that previously reported (Jacobs et al., 1989) for the MF system. AVBF binds Fe^{2+} ions in a broad, uniformly increasing pH binding profile with many more Fe^{2+} binding to AVBF at a given pH than that observed for the MF Fe^{2+}-binding reaction. The latter system binds about eight Fe^{2+}, presumably in the 3-fold channels, in a pH-independent manner from pH 6 to 7.5. Above this pH, a sharp titration-like binding profile (perhaps producing $Fe(OH)_2$) is observed. This contrasting behavior must be dictated by different structural features of the intact apo-proteins resulting from the different amino acids present and the different amino acid sequences in these two proteins. The presence of heme in AVBF clearly distinguishes this protein from MF and, although heme may be an electron-transfer agent, its presence might also be a factor in the Fe^{2+}-binding capability of apo-AVBF. The recent report of the amino acid sequence of apo-AVBF and comparisons with the sequence and structure of mammalian ferritin has allowed Grossman et al. (1992) to suggest that the heme binding site is near the inside surface of apo-AVBF. In such a position, heme could serve as an electron-transfer center and perhaps also interact with the developing mineral core.

Acknowledgments

G.D.W. and R.B.F. were supported by The National Institutes of Health (5 RO1 DK36799-05). G.C.P. was supported by the Office of Naval Research.

Registry No. Fe^{2+}, 15438-31-0; H^+, 12408-02-5; Fe^{3+}, 20074-52-6; phosphate, 14265-44-2.

References

Andrews, S. C., Harrison, P. M., & Guest, J. R. (1989) *J. Bacteriol. 171*, 3940.

Baaker, G. R., & Boyer, R. F. (1986) *J. Biol. Chem. 261*, 13182.

Bauminger, E. R., Harrison, P. M., Nowik, I., & Treffry, A. (1989) *Biochemistry 28*, 5486.

Bell, S. H., Weir, M. P., Dickson, D. P. E., Gibson, J. F., Sharp, G. A., & Peters, T. J. (1984) *Biochim. Biophys. Acta 787*, 227.

Bulen, W. A., LeComte, J. R., & Lough, S. (1973) *Biochem. Biophys. Res. Commun. 54*, 1274.

Chasteen, N. D., & Theil, E. C. (1982) *J. Biol. Chem. 257*, 7672.

Cheng, Y. G., & Chasteen, N. D. (1991) *Biochemistry 30*, 2947.

Clegg, G. A., Fitton, J. E., Harrison, P. M., & Treffry, A. (1980) *Prog. Biophys. Mol. Biol. 36*, 56.

Cooper, (1977) *Tools of Biochemistry*, p 53, John Wiley and Sons, New York.

Corbin, J. L., & Watt, G. D. (1990) *Anal. Biochem. 186*, 86.

Frankel, R. B., Papaefthymiou, G. C., & Watt, G. D. (1987) *Hyperfine Interact. 33*, 233.

Greenwood, N. N., & Gibb, T. C. (1971) *Mossbauer Spectroscopy*, p 659, Chapman and Hall, London.

Grossman, M. J., Hinton, S. M., Minak-Bernero, V., Slaughter, C., & Stiefel, E. I. (1992) *Proc. Natl. Acad. Sci. U.S.A. 89*, 2419.

Jacobs, D. L., Watt, G. D., Frankel, R. B., & Papaefthymiou, G. G. (1989) *Biochemistry 28*, 9216.

Lawson, D. M., Treffry, A., Artymuik, P. J., Harrison, P. M., Yewdall, S. J., Luzago, A., Cesareni, G., Levi, S., & Arosio, P. (1989) *FEBS Lett. 254*, 207.

Lovenberg, W. M., Buchanan, B. B., & Rabinowitz, J. C. (1963) *J. Biol. Chem. 238*, 3899.

Mann, S., Williams, J. M., Treffrey, A., & Harrison, P. M. (1987) *J. Mol. Biol. 198*, 405.

Mansour, A. N., Thompson, C., Theil, E. C., Chasteen, N. D., Moore, G. R., Mann, S., & Bannister, J. V. (1986) *J. Inorg. Biochem. 28*, 329.

Oosterhuis, W. T., & Spartalian, K. (1976) in *Applications of Mossbaurer Spectroscopy* (Cohen, R. L., Ed.) Vol. 1, pp 141-170, Academic Press, New York.

Rohrer, J. S., Islam, Q. T., Watt, G. D., Sayers, D. E., & Theil, E. C. (1990) *Biochemistry 29*, 259.

Stefanini, S., Desideri, A., Veccini, P., Drakenberg, T., & Chiancone, E. (1989) *Biochemistry 28*, 378.

Stiefel, E. I., & Watt, G. D. (1979) *Nature (London) 279*, 81.

Treffry, A., & Harrison, P. M. (1978) *Biochem. J., 171*, 313.

Wardeska, J. G., Viglione, B. J., & Chasteen, N. D. (1985) in *Proteins of Iron Storage and Transport* (Spik, G., Montrevie, J., Crichton, R. R., & Mazurier, J., Eds.) p 85, Elsevier Science, New York.

Watt, G. D., Frankel, R. B., Papaefthymiou, G. C., Spartalian, K., & Stiefel, E. I. (1986) *Biochemistry 25*, 4330.

Watt, G. D., Jacobs, D., & Frankel, R. B. (1988) *Proc. Natl. Acad. Sci. U.S.A. 85*, 7457.

Yang, C., Meagler, A., Huynh, B. H., Sayers, D. E., & Theil, E. C. (1987) *Biochemistry 26*, 497.

Yariv, J., Kalb, A. J., Sperling, R., Bauminger, E. R., Cohen, S. G., & Ofer, S. (1981) *Biochem. J. 197*, 171.